

JLab Program Advisory Committee Eleven Proposal Cover Sheet

This document must be received by close of business on Wednesday, December 18, 1996 at:

Jefferson Lab
User Liaison Office, Mail Stop 12 B
12000 Jefferson Avenue
Newport News, VA 23606

(Choose one)

~~Letter-of-Intent~~ Proposal Title: The Electric Form Factor of the Neutron Extracted from the $^4\text{He}(\vec{e}, e'n)\text{pp}$ Reaction.

Update Experiment Number: 94-021

Letter-of-Intent Title:

Contact Person

Name: W. Korsch (U.Ky.) & R. McKeown (C.I.T.)

Institution: University of Kentucky & Caltech

Address: Physics & Astronomy, Chem-Physics Bldg. (UK)

Address: Kellogg Radiation Laboratory 106-38 (Caltech)

City, State ZIP/Country: Lexington, KY 40506-0055 or
Pasadena, CA 91125

Phone: (606)257-4083 (Ky) FAX: (606)323-2846 (Ky)

E-Mail > Internet: (818)395-4316 (Ca) (818)564-8708 (Ca)

KORSCH@pa.uky.edu

BMCK@krl.caltech.edu

Experimental Hall: A Days Requested for Approval: 42

Jefferson Lab Use Only

Receipt Date: 18 DEC 96

By: L. Smith PR 96-005

HAZARD IDENTIFICATION CHECKLIST

JLab Proposal No.: 94-021
(For CEBAF User Liaison Office use only)

Date: Dec 16 1996

Check all items for which, there is an anticipated need.

<p>Cryogenics</p> <p><input type="checkbox"/> beamline magnets</p> <p><input type="checkbox"/> analysis magnets</p> <p><input type="checkbox"/> target</p> <p>type: _____</p> <p>flow rate: _____</p> <p>capacity: _____</p>	<p>Electrical Equipment</p> <p><input type="checkbox"/> cryo/electrical devices</p> <p><input type="checkbox"/> capacitor banks</p> <p><input type="checkbox"/> high voltage</p> <p><input type="checkbox"/> exposed equipment</p>	<p>Radioactive/Hazardous Materials</p> <p>List any radioactive or hazardous/toxic materials planned for use:</p> <p>_____</p> <p>_____</p> <p>_____</p>
<p>Pressure Vessels</p> <p><input type="checkbox"/> inside diameter</p> <p><input type="checkbox"/> operating pressure</p> <p><input type="checkbox"/> window material</p> <p><input type="checkbox"/> window thickness</p>	<p>Flammable Gas or Liquids</p> <p>type: _____</p> <p>flow rate: _____</p> <p>capacity: _____</p> <p>Drift Chambers</p> <p>type: _____</p> <p>flow rate: _____</p> <p>capacity: _____</p>	<p>Other Target Materials</p> <p><input type="checkbox"/> Beryllium (Be)</p> <p><input type="checkbox"/> Lithium (Li)</p> <p><input type="checkbox"/> Mercury (Hg)</p> <p><input type="checkbox"/> Lead (Pb)</p> <p><input type="checkbox"/> Tungsten (W)</p> <p><input type="checkbox"/> Uranium (U)</p> <p><input checked="" type="checkbox"/> Other (list below)</p> <p style="margin-left: 20px;"><u>3He gas, Rb, N₂</u></p> <p style="margin-left: 20px;"><u>H₂ gas</u></p>
<p>Vacuum Vessels</p> <p><input type="checkbox"/> inside diameter</p> <p><input type="checkbox"/> operating pressure</p> <p><input type="checkbox"/> window material</p> <p><input type="checkbox"/> window thickness</p>	<p>Radioactive Sources</p> <p><input type="checkbox"/> permanent installation</p> <p><input type="checkbox"/> temporary use</p> <p>type: _____</p> <p>strength: _____</p>	<p>Large Mech. Structure/System</p> <p><input type="checkbox"/> lifting devices</p> <p><input type="checkbox"/> motion controllers</p> <p><input type="checkbox"/> scaffolding or</p> <p><input type="checkbox"/> elevated platforms</p>
<p>Lasers</p> <p>type: <u>Diode Laser</u></p> <p>wattage: <u>~100W</u></p> <p>class: <u>IV</u></p> <p>Installation:</p> <p><input checked="" type="checkbox"/> permanent</p> <p><input type="checkbox"/> temporary</p> <p style="margin-left: 20px;">(For experiment)</p> <p>Use:</p> <p><input type="checkbox"/> calibration</p> <p><input type="checkbox"/> alignment</p> <p style="margin-left: 20px;">For 3He target</p>	<p>Hazardous Materials</p> <p><input type="checkbox"/> cyanide plating materials</p> <p><input type="checkbox"/> scintillation oil (from)</p> <p><input type="checkbox"/> PCBs</p> <p><input type="checkbox"/> methane</p> <p><input type="checkbox"/> TMAE</p> <p><input type="checkbox"/> TEA</p> <p><input type="checkbox"/> photographic developers</p> <p><input type="checkbox"/> other (list below)</p> <p>_____</p> <p>_____</p>	<p>General:</p> <p>Experiment Class:</p> <p><input type="checkbox"/> Base Equipment</p> <p><input type="checkbox"/> Temp. Mod. to Base Equip.</p> <p><input type="checkbox"/> Permanent Mod. to Base Equipment</p> <p><input type="checkbox"/> Major New Apparatus</p> <p>Other: _____</p> <p>_____</p>

LAB RESOURCES REQUIREMENTS LIST

Lab Proposal No.: 94-021
(For CEBAF User Liaison Office use only.)

Date: Dec, 16 1996

List below significant resources — both equipment and human — that you are requesting from JLab in support of mounting and executing the proposed experiment. Do not include items that will be routinely supplied to all running experiments, such as the base equipment for the hall and technical support for routine operation, installation, and maintenance.

Major Installations (either your equip. or new equip. requested from JLab) **Major Equipment**

Neutron Detector (array of scintillator modules)

- Request from JLab:
- support for target installation
 - working polarimeter to measure beam polarization
 - neutron detector shielding

Magnets _____

Power Supplies _____

Targets _____

Detectors Neutron Detector

Electronics _____

Computer Hardware _____

Other _____

Other

New Support Structures: _____

Data Acquisition/Reduction

Computing Resources: _____

New Software: _____

TJNAF PROPOSAL 94-021

The Electric Form Factor of the Neutron Extracted from the ${}^3\vec{\text{He}}(\vec{e}, e'n)pp$ Reaction

T. Averett, B. Filippone, E. Hughes, R. McKeown (co-spokesperson), M. Pitt

California Institute of Technology, Pasadena, CA 91101

J.P. Chen, J. Gomez, J. LeRose, R. Michaels, A. Saha

TJNAF, Newport News, VA 23606

B. Anderson, G.G. Petratos, J. Watson

Kent State University, Kent, OH 44242

W. Korsch (co-spokesperson)

University of Kentucky, Lexington, KY 40506

P. Bogorad, G.D. Cates, K. Kumar, H. Middleton

Princeton University, Princeton, NJ 08544

C. Glashauser, R. Gilman, R.D. Ransome, P. Rutt

Rutgers University, Rutgers, NJ 08855

R. Holmes, J. McCracken, P.A. Souder, X. Wang

Syracuse University, Syracuse, NY 13210

D. Kawall

Stanford University, Stanford, CA 94305

L. Auerbach, Z. Dziembowski, J. Martoff, Z.-E. Meziani, J. Park

Temple University, Philadelphia, PA 19122

I. Physics Motivation

Electron scattering has already been used for decades to measure the form factors of the proton and the neutron. The proton electric and magnetic form factors as well as the neutron magnetic form factor have been measured to high precision for Q^2 values up to several GeV^2/c^2 . However, our knowledge about the electric form factor of the neutron is quite unsatisfactory. This quantity is of fundamental theoretical interest, since it can serve as test for QCD based calculations. It is known from neutron-electron scattering that the slope of G_E^n is positive at $Q^2=0$, which implies an internal charge distribution of the neutron. So far most of the existing data on G_E^n were obtained from elastic and quasielastic scattering off deuterons. Here the model dependence of G_E^n on the deuteron wave functions is a fundamental limit for these kind of measurements. As polarized ^3He targets have become available for nuclear physics experiments, the neutron form factors can be extracted from asymmetry measurements, which are favourable over cross-section measurements, since the systematic uncertainties can be reduced significantly. Recently, a new series of measurements has been launched at different laboratories using polarized ^3He in inclusive and exclusive reactions to extract the electric and magnetic form factors of the neutron [1, 2, 3, 4, 5, 6, 7]. Especially Gao *et al.* [2] showed that polarized ^3He can be used for the extraction of G_M^n to high precision in inclusive scattering.

The first attempt to extract G_E^n by measuring the (sideways) polarization transfer to the neutron in the $d(\vec{e}, e'\vec{n})p$ reaction was performed at MIT-Bates at a Q^2 value of $0.255 \text{ GeV}^2/c^2$ [5]. This experiment allows in principle a direct way of extracting G_E^n in PWIA, when one stays in a kinematical regime where FSI and MEC contributions are kept small. However, one needs a well calibrated neutron analyzer system, to determine the polarization transfer to the neutron. This reduces the efficiency of the neutron detector. Recently, an experiment to measure G_E^n at the MAMI accelerator in Mainz using the $^3\text{He}(\vec{e}, e'n)pp$ reaction has been completed [8, 9]. This experiment was done at a low Q^2 of about $0.35 \text{ GeV}^2/c^2$. It was clearly demonstrated that the $^3\text{He}(\vec{e}, e'n)pp$ reaction is very suitable for extracting G_E^n . The limitation of this experiment was the electron spectrometry (non-magnetic spectrometer).

Therefore, we propose to measure G_E^n in Hall-A using the $^3\text{He}(\vec{e}, e'n)pp$ reaction at three different values of the 4-momentum squared, namely $Q^2 = 1 \text{ GeV}^2/c^2$, $1.5 \text{ GeV}^2/c^2$, and $2 \text{ GeV}^2/c^2$. At these high Q^2 values the effect of final state interactions (FSI) and meson exchange current contributions (MEC) are expected to be small. We certainly will verify this with state of the art calculations as already performed by a group at the University of Bochum which can perform complete FSI calculations

and is in the process of including the effect of MEC contributions [10].

We plan to use a high density polarized ${}^3\text{He}$ target together with one of the high resolution spectrometers HRS.

II. Discussion of the Experiment

We propose a set of measurements to determine the electric form factor of the neutron using the ${}^3\vec{\text{He}}(\vec{e}, e'n)\text{pp}$ reaction at three different values of Q^2 in Hall A at CEBAF. This method was first proposed by R. Arnold, C.E. Carlson, and F. Gross [11] as a polarization transfer experiment in the $d(\vec{e}, e'n)\text{p}$ reaction. Since dense polarized ${}^3\text{He}$ targets have become available the ${}^3\vec{\text{He}}(\vec{e}, e'n)\text{pp}$ reaction can also be used for the extraction of G_E^n . The ${}^3\vec{\text{He}}$ nucleus serves here as a polarized neutron. The advantage of extracting G_E^n via the ${}^3\vec{\text{He}}(\vec{e}, e'n)\text{pp}$ reaction is that one does not have to measure the polarization of the neutron in the exit channel. The efficiency of the neutron detector is therefore higher. We want to extract G_E^n for Q^2 values of 1.0, 1.5, and 2.0 GeV^2/c^2 . The scattered electrons will be detected in one of the high resolution spectrometers (HRS) and for neutron detection we plan to build a special detector array with a total active area of $120 \times 120 \text{ cm}^2$ and a thickness of about 10 cm per layer (total thickness 30 cm). The neutron detector will be built by our collaborators from KSU [12]. A detailed description of the neutron detector is given below. The measured asymmetry for the ${}^3\vec{\text{He}}(\vec{e}, e'n)\text{pp}$ reaction can be expressed as follows in PWIA:

$$A = -P_e P_n D \left\{ \frac{2\sqrt{\tau(\tau+1)}\tan(\vartheta_e/2)G_E^n G_M^n \sin(\theta^*) \cos(\phi^*)}{G_E^{n2} + G_M^{n2}(\tau + 2\tau(1+\tau)\tan^2(\vartheta_e/2))} + \frac{2\tau\sqrt{1+\tau + (1+\tau)^2\tan^2(\vartheta_e/2)}\tan(\vartheta_e/2)G_M^{n2} \cos(\theta^*)}{G_E^{n2} + G_M^{n2}(\tau + 2\tau(1+\tau)\tan^2(\vartheta_e/2))} \right\}. \quad (1)$$

Here P_e is the electron polarization, P_n is the neutron polarization, D is an overall dilution factor which contains dilution from (possible) unpolarized neutrons in the target and dilution from background neutrons generated in (p,n) reactions, e.g. in shielding walls. $\tau = (Q^2/4 m_n^2)$, ϑ_e is the electron scattering angle, G_E^n and G_M^n are the neutron electric and magnetic form factors, respectively, θ^* is the polar angle of the ${}^3\text{He}$ spin vector relative to the q_3 vector, and ϕ^* is the azimuthal angle of the target spin vector relative to the scattering plane. Eqn. 1 shows the obvious sensitivity to G_E^n in the longitudinal-transversal interference term. Therefore, by aligning the target spin perpendicular to \vec{q} , i.e. choosing θ^* equals 90° , and ϕ^* equals

0° the above equation can be rewritten in the following form:

$$G_e^n = -\frac{A_{perp}}{P_e P_n D} \cdot \frac{G_M^n (\tau + 2\tau(1 + \tau)\tan^2(\vartheta_e/2))}{2\sqrt{\tau(1 + \tau)}\tan(\vartheta_e/2)}. \quad (2)$$

Aligning the target spin parallel to \vec{q} reduces Eqn 2 to ($G_E^n \approx 0$):

$$A_{long} = -P_e P_n D \frac{2\sqrt{1 + \tau + (1 + \tau)^2 \tan^2(\vartheta_e/2)}\tan(\vartheta_e/2)}{1 + 2(1 + \tau)\tan^2(\vartheta_e/2)}. \quad (3)$$

This equation is completely independent of the neutron form factors and serves as an excellent calibration reaction. Combining Equations 2 and 3 gives

$$G_E^n = \sqrt{\tau + \tau(1 + \tau)\tan^2(\vartheta_e/2)} \frac{A_{perp}}{A_{long}} G_M^n. \quad (4)$$

In principal Eqn.2 as well as Eqn.4 can be used to extract G_E^n , but it is obvious that the systematic error which is attached to Eqn.4 is smaller than in Eqn.2. Therefore we want to use Eqn.4 to extract G_E^n , especially, since it will be shown that A_{long} can be measured to a good precision in a relatively short time. Table 1 lists the values for G_E^n in Galster parameterization [13], G_M^n in dipole parameterization, and the longitudinal and perpendicular asymmetries (physics asymmetries) for our three Q^2 values.

TABLE 1 G_E^n in Galster parameterization, G_M^n in dipole parameterization, A_{perp}^{phys} , and A_{long}^{phys} for the three different values of Q^2 . Here we have $P_n = P_e = D = 1$.

Q^2 [GeV ² /c ²]	G_E^n	G_M^n	A_{perp}	A_{long}
1.0	$3.61 \cdot 10^{-2}$	0.329	$-5.83 \cdot 10^{-2}$	-0.286
1.5	$2.48 \cdot 10^{-2}$	0.197	$-7.21 \cdot 10^{-2}$	-0.382
2.0	$1.78 \cdot 10^{-2}$	0.131	$-8.17 \cdot 10^{-2}$	-0.469

It is obvious from the table that the longitudinal asymmetries are a factor of 5-6 larger than the perpendicular asymmetries.

III. Rate and Background Estimates

The idea of the experiment is to extract G_E^n in quasi-elastic kinematics at a beam energy of 4 GeV and Q^2 values of 1, 1.5, and 2 GeV^2/c^2 . We assume a beam current of 15 μA with a polarization of 0.8. Such high beam polarizations have been already achieved at SLAC with quantum efficiencies of 0.1-0.3 %.

The polarized ^3He target will be very similar to the ones used in the E142/154 experiments at SLAC (see section VI.) We plan to use a target with a ^3He volume density of $2.5 \cdot 10^{20}$ atoms/ cm^3 . Since we are going to use technique of collisional spin-exchange with optically pumped Rb, there will be a Rb density of the order $6 \cdot 10^{14}$ atoms/ cm^3 as well as a partial pressure of about 100 torr (or $1.4 \cdot 10^{19}$ N/ cm^3) at room temperature in the target. The Rb and N atoms contain (unpolarized) neutrons which will amount in a dilution factor of 0.94 (ratio of the total number of ^3He neutrons to the total number of neutrons in the target). The length of the target will be 40 cm with a polarization of about 0.45. Table 2 summarizes some kinematical parameters for the three different values of Q^2 .

TABLE 2 *Experimental parameters for the three different Q^2 settings at an incident beam energy of 4 GeV. The effective target length was taken to be $10\text{cm}/\sin(\vartheta_e)$.*

Q^2 [GeV^2/c^2]	ϑ_e [$^\circ$]	ϑ_q [$^\circ$]	E' [GeV]	eff. tgt. length [cm]	tgt. density [cm^{-2}]
1.0	15.5	54.3	3.463	37.4	$9.4 \cdot 10^{21}$
1.5	20	47.1	3.182	29.2	$7.3 \cdot 10^{21}$
2.0	24	41.8	2.923	24.6	$6.1 \cdot 10^{21}$

The estimates for the reaction rates were performed with a Monte Carlo code which is a modified version of the EGPN code developed by van den Brand [14]. The cross-sections were calculated in PWIA with de Forest's CC1 off-shell description [15] and the ^3He wave function generated by Schulze and Sauer [16]. We used a pointlike target in our calculation. The acceptances of the HRS are ± 30 mr in the horizontal plane and ± 65 mr in the vertical plane. The total solid angle for the electron arm is therefore 7.8 msr. The momentum acceptance $\Delta p/p$ of the HRS is 10% and the transverse length acceptance is 10 cm. As mentioned above the neutron detector will have an active area of 120×120 cm^2 with a total neutron detection efficiency of about 0.12 (see section V.) The detector will be positioned about 16 m away from the target at a Q^2 of 1 GeV^2/c^2 and about 20 m away for the Q^2 values of 1.5 and 2.0 GeV^2/c^2 . This ensures that we have enough timing resolution ($\approx 1\text{ns}$) to

distinguish between quasi-elastically scattered neutrons and neutrons associated with pion production. The solid angle is about 6 msr for the low Q^2 value and 3.6 msr for the two higher Q^2 . The solid angle is purposely kept small (up to about 50 MeV/c transverse momentum), to keep the background low and to keep the kinematics close to the quasielastic peak. In order to distinguish charged particles from the neutrons, we will add thin ΔE scintillators in front of the the neutron detector. The whole neutron detector will be enclosed in a concrete shielding hut to suppress low energetic electromagnetic background. The entrance window will be made of an about 10 cm thick Pb wall. Therefore, one possible source of background neutrons can be due to (p,n) reactions in the Pb. In order to estimate the size of this dilution factor a Monte Carlo Simulation was performed where we assumed that protons (pencil beam) with kinetic energies of 500 MeV and 1000 MeV (monoenergetic) hit the center of a 120×120 cm² Pb wall with a thickness of 10 cm and 20 cm. The neutron detector was placed 1 m downstream. All neutrons that emerged from the Pb wall and hit the detector were recorded. The calculations were performed at Los Alamos using the LAHET Monte Carlo code [17]. The LAHET program is a transport and interaction code for nucleons, pions, muons, light ions, and antinucleons in complex geometry. The code is a modified version of the LANL-HETC code and has its special application in high energy (up to several GeV) reactions. The result of the calculations is shown in Table 3.

TABLE 3 *Neutron yield from the Pb(p,n) reaction with proton energies of 500 MeV and 1000 MeV.*

E_{neut} [MeV]	10 cm Pb	10 cm Pb	20 cm Pb	20 cm Pb
	500 MeV p	1000 MeV p	500 MeV p	1000 MeV p
	# neut./inc.prot.	# neut./inc.prot.	# neut./inc.prot.	# neut./inc.prot.
0-30	0.0093	0.024	0.0116	0.0302
30-50	0.0125	0.024	0.0135	0.0355
50-70	0.0098	0.018	0.0132	0.0242
70-90	0.0080	0.013	0.0088	0.0200
90-100	0.0035	0.008	0.0047	0.0070
100-300	0.0035	0.053	0.0438	0.0838
300-500	0.0168	0.027	0.0097	0.0315
500-1000	–	0.025	–	0.0258

For our proposed kinematics the typical nucleon kinetic energies are 537 MeV, 818 MeV, and 1077 MeV at the three Q^2 values, for nucleons knocked out at the quasi-elastic peak. Therefore, the only relevant rows in the above table are the

neutron energy ranges 300-500 MeV and 500-1000 MeV. All the lower energies can be discriminated by setting proper detector thresholds or moving the Pb shielding wall closer to the target and use TOF discrimination.

Table 4 lists the estimated proton and neutron rates which will be accepted by the solid angle of the neutron detector. By means of rows 7 and 8 from Table 3 the dilution factor ($=\frac{S}{S+B}$, where S denotes the real neutron events and B neutrons generated in the Pb wall) is shown as well.

TABLE 4 *Estimated proton and neutron rates in the solid angle of the neutron detector. The proton rates are the sums of the rates coming from 2-body and 3-body ^3He break-up. The neutron rates induced by the $\text{Pb}(p,n)$ reaction and the dilution factor ($=S/(S+B)$) are also shown.*

Q^2 [GeV ² /c ²]	Signal n-Rate [Hz]	p-Rate [Hz]	Background n-Rate [Hz]	D
1	29.1	194.7	3.3	0.90
1.5	3.2	14.7	0.5	0.87
2	0.87	3.61	0.13	0.87

These estimates show that the dilution due to the (p,n) conversion in Pb is of the order 10-15%. We intend to measure the background directly by using a hydrogen filled target cell.

Background contributions due to beam - glass cell interactions will be minimized by collimating out the end windows of the cell on both detector sides (HRS and neutron detector).

In addition we would like to mention, that the protons in polarized ^3He have a small probability of being in the spatially mixed symmetric S' state (about 2-3%) and about 10% probability of being in a relative D-state. This leads to an effective proton polarization of about 10%, which will induce an asymmetry in the background. Asymmetry calculations for the $^3\vec{\text{He}}(\vec{e}, e'p)d$ reaction from Laget at a Q^2 predict asymmetries on the order of about 5-10% at small missing momentum. Our main contribution of background protons comes from the 2-body breakup reaction, only about 30% of the total proton rate comes from 3-body breakup in our kinematics. Using this information the estimated asymmetry in the background is about 0.02-0.03%. These asymmetries are about 2 orders of magnitude smaller than the expected asymmetries from the $^3\vec{\text{He}}\vec{e}, e'n)pp$ reaction and can be neglected within the precession of this experiment.

Another possible source of background are inelastic events coming from single pion production. In order to get an estimate of the inclusive yield in the electron spectrometer that corresponds to non-quasielastic events we used the inclusive ^3He spectra from Day *et al.* at the Q^2 values of 1 and 2 GeV^2/c^2 . Day *et al.* also show the result of a Fadeev calculation for the quasi-elastic yield. If we use the 10 % momentum bite of the HRS we can estimate the excess yield of events coming from the high energy-loss side of the quasi-elastic peak. We assign the excess yield, compared to the Fadeev calculation, to inelastic events. The relative fraction coming from these events is about 0.15 at a Q^2 of 1 GeV^2/c^2 and 0.2 at $Q^2 = 2 \text{ GeV}^2/c^2$.

We also take into account the inelastically generated neutrons have on average much larger transverse momenta ($>100 \text{ MeV}/c$) than neutrons with a typical Fermi motion of ^3He (about $50 \text{ MeV}/c$). This effect leads to a reduction of the solid angle for inelastic neutrons, since $\Delta\vartheta_{qn}$ is larger. We estimate the fraction of inelastically generated neutrons in the solid angle of our neutron detector is 0.055 ($Q^2=1 \text{ GeV}^2/c^2$) and 0.067 ($Q^2=2 \text{ GeV}^2/c^2$).

Finally we considered the effect of the TOF cut, which is a cut on the missing energy. We use a fit to the $F(y)$ scaling function obtained from the Day *et al.* data and assume that the pion is produced through Δ dominance. Now we can estimate the fraction of inelastically produced neutrons in the acceptance of our solid angle and determine its missing energy spectrum. Due to the long flight paths (16 m and 20 m) we will have a TOF energy resolution of 31 MeV for $Q^2=1 \text{ GeV}^2/c^2$, 56 MeV for $Q^2=1.5 \text{ GeV}^2/c^2$, and 97 MeV for $Q^2=2 \text{ GeV}^2/c^2$ assuming a timing resolution Δt of 1 ns. If we now require a missing energy cut of 100 MeV the fraction of inelastically generated neutrons is 0.07 for the low Q^2 value and 0.11 for the highest Q^2 value.

Multiplying the 3 different relative yields amounts to a neutron background due to pion production of the order 0.1%. Even if these estimates are off by a factor of 2, it is clear, that the neutron background from inelastic events is negligible.

IV. The Neutron Detector

At present we have 12 scintillator detectors with the dimension of $1.0 \times 0.25 \times 0.1$ m³ and 3 scintillators with the dimensions of $1 \text{m} \times 0.5 \times 0.1$ m³. This would allow us to set up a neutron detector with an active area of 1.5×1.0 m² and a total thickness of 0.3 m. We consider this geometry as a fall back situation, our goal is to build a neutron detector with the above proposed active area of 1.2×1.2 m². We will start to pursue this as soon as this proposal gets fully approved.

The neutrons will be detected in coincidence with an array of plastic scintillator neutron counters. Each scintillator has a tapered lucite light pipe mounted on each end viewed by a 5in PMT. The detector uses the signals from each end to obtain a mean-timed fast timing signal, the position signal, and the summed pulse height. The intrinsic time resolution of these detectors is 200 ps, measured with cosmic rays and verified at accelerator experiments. The array will be formed as three layers of five detectors each. The estimated efficiency from Monte Carlo simulations is about 8% for 1 GeV neutrons for each layer. The total efficiency is then about 24%.

The neutron detector array must be placed in a shielding hut to protect it from the large photon flux that will be present. Based on an earlier experiment at the Bates laboratory, at least 4 feet of high density concrete is required to surround the array in order to fully attenuate the photon flux and room scattered neutrons. A window needs to be placed in this shielding on the target side to allow the neutrons of interest to enter the array. This window needs to be a lead wall (about 10 cm thick). This wall will degrade all gamma rays to below the detector thresholds so that only neutrons will be detected. The lead will also attenuate the neutrons by about 50%; hence the overall efficiency of the detector array is about 12% percent.

V. Extraction of G_E^n

Based on the assumptions from the previous chapters we get counting rates and accuracies as shown in Table 5.

TABLE 5 *Estimated rates and accuracies for the perpendicular asymmetry. We assume a ^3He polarization of 0.45, a beam polarization of 0.8, and a neutron detection efficiency ϵ of 0.12. The dilution factor is the product of 0.94 and the $S/(S+B)$ ratio from above. The asymmetries were estimated using the dipole parameterization for G_M^n and the Galster parameterization for G_E^n*

Q^2 [GeV $^2/c^2$]	Rate [s $^{-1}$]	D	Rate $\cdot\epsilon$ [s $^{-1}$]	N_{tot} (10 days)	$\Delta A = \frac{1}{\sqrt{N}}$ (10 days)	A_{perp}^{meas} [%]	$\frac{\Delta A}{A_{perp}}$ [%]
1.0	29.1	0.85	3.5	$3.02 \cdot 10^6$	$5.75 \cdot 10^{-4}$	-1.54	3.7
1.5	3.2	0.81	0.38	$3.28 \cdot 10^5$	-1.83	$1.75 \cdot 10^{-3}$	9.6
2.0	0.87	0.81	0.10	$8.64 \cdot 10^4$	-2.09	$3.40 \cdot 10^{-3}$	16.2

Similarly, Table 6 displays the longitudinal asymmetry when G_E^n is set to be equals zero.

TABLE 6 *Estimated rates and accuracies for the longitudinal asymmetry. Same assumptions as in Table 3*

Q^2 [GeV $^2/c^2$]	τ	ϑ_e [$^\circ$]	N_{tot} (1 day)	A_{long} [%]	$\frac{\Delta A}{A_{long}}$ (1 day) [%]
1.0	0.286	15.5	$3.02 \cdot 10^5$	- 7.89	2.3
1.5	0.435	20.0	$3.28 \cdot 10^4$	- 10.00	5.5
2.0	0.573	24.0	$8.64 \cdot 10^3$	- 12.36	8.7

For an estimate of the systematic error we assume the following relative accuracies for the beam energy: $5 \cdot 10^{-4}$, the scattered electron energy: $1 \cdot 10^{-4}$, G_M^n : 0.05 [18], and if further the electron scattering angle to ± 2 mr, we will end up with an error of about 5%. One additional source of a systemtic error is the knowledge of the polarization angles ϑ^* and ϕ^* . Since we plan to use $\phi^* = 0^\circ$, it is clear from Eqn. 1 that the effect on the (perpendicular) asymmetry goes like $\cos(\phi^*)$ and a small misalignment of the spin in ϕ^* will have a negligible effect. Our goal is to orient the spin better than $\pm 0.5^\circ$ in ϑ^* and ϕ^* . It is also obvious from Eqn. 1 that the longitudinal asymmetry is also insensitive to misalignments, but there is some sensitivity to the perpendicular asymmetry, since here ϑ^* enters with $\sin(\vartheta^*)$. A

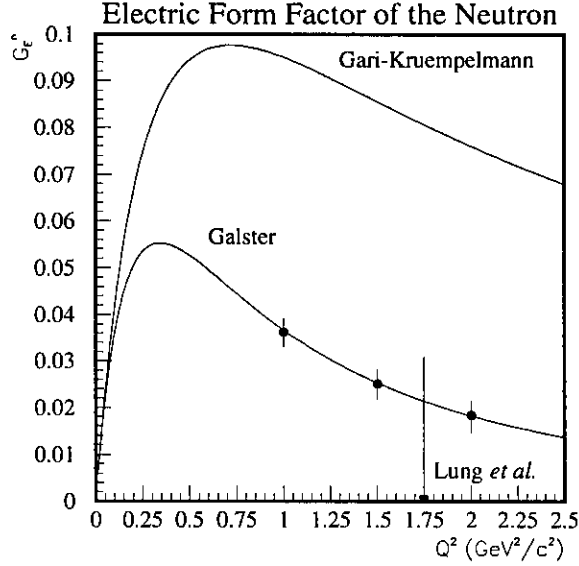


Figure 1: G_E^n as a function of Q^2 . The solid curve corresponds to the Galster parameterization and the dashed-dotted curve to a parameterization given by Gari and Krümpelmann. Shown are the projected error bars of the proposed experiment as well as the data point from Lung et al.

misalignment of $\pm 0.5^\circ$ will introduce an additional relative error of about 5%. The major contribution to the systematic error is the error in G_M^n . Systematic errors in the determination of beam - and target polarizations cancel since we use the ratio A_{perp}/A_{long} for extracting G_E^n . The amounting total errors in the extraction of G_E^n are listed in Table 7 and Fig.1 shows the error bars as compared to the Galster parameterization of G_E^n .

TABLE 7 Total fractional errors for the extraction of G_E^n . Here the G_E^n values in the Galster parameterization were used. All error contributions were added in quadrature

Q^2 [GeV ² /c ²]	$\frac{\Delta G_E^n}{G_E^{Galster}}$ [%]
1.0	± 8.3
1.5	± 13.1
2.0	± 19.7

VI. The Polarized ^3He Target

The polarized target will be based on the principle of spin exchange between optically pumped alkali-metal vapor and noble-gas nuclei [20, 21, 22]). The design will be similar in many ways to that used in E-142, an experiment at SLAC to measure the spin dependent structure function of the neutron [23]. A central feature of the target will be sealed glass target cells, which will contain a ^3He pressure of about 10 atmospheres. As indicated in Fig.2, the cells will have two chambers, an upper chamber in which the spin exchange takes place, and a lower chamber, through which the electron beam will pass. In order to maintain the appropriate number density of alkali-metal (which will probably be Rb) the upper chamber will be kept at a temperature of 170–200°C using an oven constructed of the high temperature plastic Torlon. With a density of 2.5×10^{20} atoms/cm³, and a lower cell length of 40 cm, the target thickness will be 1.0×10^{22} atoms/cm².

We describe below in greater detail some features of the target.

1 Operating Principles

The time evolution of the ^3He polarization can be calculated from a simple analysis of spin-exchange and ^3He nuclear relaxation rates [24]. Assuming the ^3He polarization $P_{^3\text{He}} = 0$ at $t = 0$,

$$P_{^3\text{He}}(t) = \langle P_{\text{Rb}} \rangle \left(\frac{\gamma_{\text{SE}}}{\gamma_{\text{SE}} + \Gamma_{\text{R}}} \right) \left(1 - e^{-(\gamma_{\text{SE}} + \Gamma_{\text{R}})t} \right), \quad (5)$$

where γ_{SE} is the spin-exchange rate per ^3He atom between the Rb and ^3He , Γ_{R} is the relaxation rate of the ^3He nuclear polarization through all channels other than spin exchange with Rb, and $\langle P_{\text{Rb}} \rangle$ is the average polarization of a Rb atom. Likewise, if the optical pumping is turned off at $t = 0$ with $P_{^3\text{He}} = P_0$, the ^3He nuclear polarization will decay according to

$$P_{^3\text{He}}(t) = P_0 e^{-(\gamma_{\text{SE}} + \Gamma_{\text{R}})t}. \quad (6)$$

The spin exchange rate γ_{SE} is defined by

$$\gamma_{\text{SE}} \equiv \langle \sigma_{\text{SE}} v \rangle [\text{Rb}]_{\text{A}} \quad (7)$$

where, $\langle \sigma_{\text{SE}} v \rangle = 1.2 \times 10^{-19}$ cm³/sec is the velocity-averaged spin-exchange cross section for Rb– ^3He collisions([24, 25, 26]) and $[\text{Rb}]_{\text{A}}$ is the average Rb number

density seen by a ^3He atom. Our target will be designed to operate with $1/\gamma_{\text{SE}} = 8$ hours.

From Eq. (6) it is clear that there are two things we can do to get the best possible ^3He polarization — maximize γ_{SE} and minimize Γ_{R} . But from Eq. (7) it is also clear that maximizing γ_{SE} means increasing the alkali-metal number density, which in turn means more laser power. The number of photons needed per second must compensate for the spin relaxation of Rb spins. In order to achieve $1/\gamma_{\text{SE}} = 8$ hours, we will require about 24 Watts of usable laser light at a wavelength of 795 nm. We will say more about the source of laser light below.

The rate at which polarization is lost, which is characterized by Γ_{R} , will have four principle contributions. An average electron beam current of about $15 \mu\text{A}$ will result in a depolarization rate of $\Gamma_{\text{beam}} = 1/30$ hours [27]. Judging from experience at SLAC, we can produce target cells with an intrinsic rate of $\Gamma_{\text{cell}} = 1/50$ hours. This has two contributions, relaxation that occurs during collisions of ^3He atoms due to dipole-dipole interactions [28], and relaxation that is presumably due largely to the interaction of the ^3He atoms with the walls. Finally, relaxation due to magnetic field inhomogeneities can probably be held to about $\Gamma_{\nabla B} = 1/100$ hours [29]. Collectively, under operating conditions, we would thus expect

$$\Gamma_{\text{R}} = \Gamma_{\text{beam}} + \Gamma_{\text{cell}} + \Gamma_{\nabla B} = 1/30 \text{ hours} + 1/50 \text{ hours} + 1/100 \text{ hours} = 1/16 \text{ hours} . \quad (8)$$

Thus, according to Eq. 5, the target polarization cannot be expected to exceed

$$P_{\text{max}} = \frac{\gamma_{\text{SE}}}{\gamma_{\text{SE}} + \Gamma} = 0.66 . \quad (9)$$

Realistically, we will not achieve a Rb polarization of 100% in the pumping chamber, which will reduce the polarization to about 45–50%.

2 Target Cells

The construction and filling of the target cells must be accomplished with great care if $1/\Gamma_{\text{cell}}$ is to be in excess of 50 hours. We plan to use the “Princeton Prescription” which was developed for use in SLAC E-142. This resulted, among the cells that were tested, in lifetimes that were always better than 30 hours, and in about 60% of the cells, better than 50 hours. The following precautions will be taken:

- 1. Cells will be constructed from aluminosilicate glass.
- 2. All tubing will be “resized.” This is a process in which the diameter of the tubing is enlarged by roughly a factor of two in order to insure a smooth pristine glass surface that is free of chemical impurities.

- 3. Cells will be subjected to a long (4-7 day) bake-out at high ($> 400^{\circ}\text{C}$) temperature on a high vacuum system before filling.
- 4. Rb will be doubly distilled in such a manner as to avoid introducing any contaminants to the system.
- 5. The ^3He will be purified either by getters or a liquid ^4He trap during filling.

The cells will be filled to a high density of ^3He by maintaining the cell at a temperature of about 20 K during the filling process. This is necessary so that the *pressure* in the cell is below one atmosphere when the glass tube through which the cell is filled is sealed.

The length of the cell has been chosen to be 40 cm so that the end windows will not be within the acceptance of the Hall A spectrometers. The end windows themselves will be about $100\ \mu$ thick. Thinner windows could in principle be used, but this does not appear to be necessary.

3 The Optics System

As mentioned above, approximately 20-24 Watts of “usable” light at 795 nm will be required. By “usable,” we essentially mean light that can be readily absorbed by the Rb. It should be noted that the absorption line of the Rb will have a full width of several hundred GHz at the high pressures of ^3He at which we will operate. Furthermore, since we will operate with very high Rb number densities that are optically quite thick, quite a bit of light that is not within the absorption linewidth is still absorbed.

It is our plan to take advantage of new emerging diode laser technology to economically pump the target. Systems are now commercially available in which a single chip produces about 20 watts of light, about half of which is probably usable. Between 2-4 such systems, at a cost of about \$25,000 each, should do the job. There is also a group at Lawrence Livermore Laboratory that has offered to build us a single chip that can produce 150 watts. While some studies of the use of diode lasers for spin-exchange optical pumping do exist in the literature [30], actual demonstrations of high polarizations in cells suitable for targets are much more recent [31]. It is our opinion that diode lasers will probably work, but we will perform several tests before freezing this decision.

At SLAC, five titanium-sapphire/argon ion laser systems were used to drive the E-142 polarized ^3He target. This option will definitely work, but is much more expensive.

4 Polarimetry

Polarimetry will be accomplished by two means. During the experiment, polarization will be monitored using the NMR technique of adiabatic fast passage (AFP) [32]. The signals will be calibrated by comparing the ^3He NMR signals with those of water. The calibration will be independently verified by studying the frequency shifts that the polarized ^3He nuclei cause on the electron paramagnetic resonance (EPR) lines of Rb atoms [27]. This second techniques will be performed in separate target studies, not during the experiment. It will serve solely as a check of our calibration. We plan to determine the polarization of the target to within 5% of itself.

5 Apparatus Overview

The target will be in air or, perhaps, in a helium bag. This greatly simplifies the design. The main components of the target are shown in Fig.2.

The “main coils” shown are large Helmholtz coils that will be used to apply a static magnetic field of about 20 Gauss. In addition to establishing the quantization axis for the target, the main coils are important for suppressing relaxation due to magnetic field inhomogeneities, which go like $1/B^2$. At 20 G, inhomogeneities can be as large as about 30 mG/cm while keeping $\Gamma_{\nabla B} < 1/100\text{hours}$. By increasing the applied field to about 40 G, and relaxing our requirements on $\Gamma_{\nabla B}$ by about factor of two, inhomogeneities as large as 0.25 G/cm can be tolerated. We are still finalizing our final choice of static field.

The NMR components in the target include a set of RF drive coils, and a separate set of pick-up coils. Not shown in the figure are the NMR electronics, which include an RF power amplifier, a lock-in amplifier, some bridge circuitry, and the capability to sweep the static magnetic field.

The oven shown in Fig.2 is constructed of Torlon, a high temperature plastic. The oven is heated with forced hot air.

The optics system will either include five Ti:sapphire lasers (only one is shown) or 2-4 laser diode systems. Either way, there will also be several lenses and a quarter wave plate to provide circular polarization.

VII. Contribution of the Collaboration and Beam Time Request

It has been shown in the previous chapters that the ${}^3\vec{\text{H}}\text{e}(\vec{e}, e'n)\text{pp}$ reaction is a very powerful tool to extract G_E^n . The contribution of the collaboration to the experiment will be:

- Construction and installation of the polarized ${}^3\text{He}$ target. This includes Helmholtz coils for the target guiding field and target polarimeter.
- Construction of the neutron detector.

We request from CEBAF:

- Polarized beam of $15\mu\text{A}$ and a beam polarization of 80% at a beam energy of 4 GeV.
- Support for target installation.
- Beam pipe instrumentation, i.e. beam position and beam current monitors.
- Working polarimeter to measure the beam polarization.
- Neutron detector shielding.

(We would like to note that this experiment only requires that 1 HRS spectrometer be operational in Hall A.)

Further we request a total running time of 1000 hrs to perform the complete experiment. We will need 800 hrs for the production run, about 70 hrs for beam polarization measurements (about 2 hours per day), 10% of the data taking for background studies, i.e. 80 hrs, and 50 hrs for moving of the spectrometers and neutron detector with shielding.

References

References

- [1] J.L. Friar *et al.*, *Phys. Rev. C* **42**, 2310 (1990).
- [2] H. Gao *et al.*, *Phys. Rev. C* **50**, R546 (1994).
- [3] C. Jones *et al.*, *Phys. Rev. C* **47**, 110 (1993).
- [4] T.E. Chupp *et al.*, *Phys. Rev. C* **45**, 915 (1992).
- [5] T. Eden *et al.*, *Phys. Rev. C* **50**, R1749 (1994).
- [6] E.E. Bruins *et al.*, *Phys. Rev. Lett.* **75**, 21 (1995).
- [7] P. Markowitz *et al.*, *Phys. Rev. C* **48**, R5 (1993).
- [8] J. Becker *et al.*, proceedings of the international workshop on “Polarized Beams and Polarized Gas Targets”, Cologne 1995, Editors H.P. gen. Schieck and L. Sydow, World Scientific.
- [9] M. Meyerhoff *et al.*, *Phys. Lett. B* **327**, 201 (1994).
- [10] J. Golak, S. Ishikawa, and W. Glöckle, private communication.
- [11] R.G. Arnold *et al.*, *Phys. Rev. C* **23**, 363 (1981).
- [12] “Neutron Detection Systems for CEBAF”, J.W. Watson, Research Program at CEBAF (III) (1987).
- [13] S. Galster *et al.*, *Nucl. Phys. B* **32**, 221 (1971).
- [14] J.v.d. Brand, private communication.
- [15] T. de Forest, *Nucl. Phys. A* **392**, 232 (1983).
- [16] R.W. Schulze and P.U. Sauer, *Phys. Rev. C* **48**, 38 (1993).
- [17] D. Lee, private communication.
- [18] A. Lung *et al.*, *Phys. Rev. Lett.* **70**, 718 (1993).
- [19] M.F. Gari and W. Krümpelmann, *Z. Phys. A* **322**, 689 (1985).
- [20] M.A. Bouchiat, T.R. Carver and C.M. Varnum, *Phys. Rev. Lett.* **5**, 373 (1960).

- [21] N.D. Bhaskar, W. Happer, and T. McClelland, *Phys. Rev. Lett.* **49**, 25 (1982).
- [22] W. Happer, E. Miron, S. Schaefer, D. Schreiber, W.A. van Wijngaarden, and X. Zeng, *Phys. Rev. A* **29**, 3092 (1984).
- [23] E142 Collaboration, P.L Anthony *et al.*, *Phys. Rev. Lett.* **71**, 959 (1993).
- [24] T.E. Chupp, M.E. Wagshul, K.P. Coulter, A.B. McDonald, and W. Happer, *Phys. Rev. C* **36**, 2244 (1987).
- [25] K.P. Coulter, A.B. McDonald, W. Happer, T. E. Chupp, and M.E. Wagshul, *Nucl. Instrum. Methods A* **270**, 90 (1988).
- [26] N.R. Newbury, A.S. Barton, P. Bogorad, G. D. Cates, M. Gatzke, H. Mabuchi, and B. Saam, *Phys. Rev. A* **48**, 558 (1993).
- [27] K.P. Coulter, A.B. McDonald, G.D. Cates, W. Happer, T.E. Chupp, *Nucl. Instrum. Methods A* **276**, 29 (1989).
- [28] N. R. Newbury, A. S. Barton, G. D. Cates, W. Happer, and H. Middleton, *Phys. Rev. A* **48**, 4411 (1993).
- [29] G.D. Cates, S.R. Schaefer and W. Happer, *Phys. Rev. A* **37**, 2877 (1988); G.D. Cates, D.J. White, Ting-Ray Chien, S.R. Schaefer and W. Happer, *Phys. Rev. A* **38**, 5092 (1988).
- [30] M. E. Wagshul and T. E. Chupp, *Phys. Rev. A* **40**, 4447 (1989).
- [31] B. Cummings, private communication.
- [32] A. Abragam, Principles of Nuclear Magnetism (Oxford University Press, New York, 1961).